



Fine-Scale P- and S-Wave Velocities From Elastic Full Waveform Inversion of Multi-Component and Time-Lapse Data: Future of Quantitative Seismic Imaging

Satish Singh* (IPG Paris, France, singh@ipgp.jussieu.fr), **Tim Sears** (British Gas, UK), Mark Roberts (IPG Paris, France), **Adam Gosselet** (IPG Paris, France), **Penny Baton** (University of Cambridge, UK)

Summary

Conventional method of seismic data analyses provide high-quality seismic image, but the image remains qualitative. Elastic full waveform inversion can provide quantitative measure of elastic parameters, which can be used to quantify the lithology, fluid and gas content, and excess pressure. Both travel-time and amplitude information within shot domain data are used to invert for the sub-surface velocity, from a starting model containing the long wavelength features. Although full waveform inversion is computationally intense, the ability to invert for both P- and S-wave velocity, in a data driven manner, makes the computational burden worthwhile. Over the last ten years, we have developed a suite of full waveform inversion algorithm and have applied to multi-component ocean bottom cable data from the North Sea to quantify gas clouds, walk-away VSP data from the Gulf of Mexico to determine the presence over-pressure beneath a salt dome, and to quantify sequestered CO₂ in the time-lapse mode. We demonstrate that the waveform inversion can indeed provide P and S-wave velocities on metric-scale and can quantify thin layers of gas or CO₂, over pressure region etc, and should be used prior to expensive drilling.

Introduction

Seismic reflection data are acquired at a very high cost. Conventional processing (stacking and migration) provides very high-quality image of the sub-surface, but does not provide any quantitative measure of the physical properties of the sub-surface. Amplitude versus offset (AVO) analyses can be used to estimate P and S-wave impedances. Since the method is local, i.e. assumes 1D media, linear approximation to the reflection coefficient, and ignores interference effects, the results are very approximative. Over the last ten years, we have developed a suite of 1D and 2D full waveform inversion. The 1D inversion was very successful and we applied to gas hydrate and magma chamber reflections (Singh et al., 1993; Singh et al., 1998). We extended the method to 2D and applied to streamer data (Shipp and Singh, 2002), using the pressure wavefield data to invert the P-wave velocity. Of particular interest in this work was the use of wide-aperture data, containing near-

and post-critical angle reflections, which helped to constrain essential medium scale features of the velocity model, allowing convergence towards the global minimum. We extended this method to invert for both P- and S-wave velocities (V_p and V_s), using the recorded wavefield at the seafloor, now readily acquired by means of multi-component ocean-bottom cable (OBC) technology or in bore holes using vertical array of geophones. Vertical (V_z) and horizontal (V_x) particle velocity records are considered, allowing both P- and S-waves (mode-converted waves) to be exploited.

The elastic waveform inversion scheme used here is adapted from the work by Shipp and Singh (2002) and Freudenreich et al. (2002), based on the theoretical framework of Tarantola (1986). The scheme is based on a finite-difference solution to the 2D elastic wave equation (Levander, 1988), operating in the time-distance domain. The aim of the scheme is to model shot gathers accurately,



and to use the residual between observed and modeled wavefields to update the velocity model appropriately. Gradients are conditioned by means of the conjugate gradient method. Both V_p and V_s may be inverted for, whilst density is coupled empirically with V_p .

Misfit Function

Full waveform inversion is formulated so that it makes few assumptions about ray paths or the media through, which the waveforms are traveling and seeks to extract all the information contained in the waveforms (both amplitude and phase). It is therefore a powerful tool that can be applied in many areas of structural complexity, such as salt domes or gas clouds, where many other conventional processing methods may break down due to the assumptions made and the lack of a data driven approach.

In pre-stack full waveform inversion we minimize a misfit function $S(d_{obs,m})$ defined here as the difference between the observed (d_{obs}) and modeled (d_{syn}) data (the misfit), in a least squares sense:

$$S(d_{obs,m}) = (d_{syn} - d_{obs})^T C_d^{-1} (d_{syn} - d_{obs}),$$

where C_d is the data covariance matrix, which is assumed to be the identity matrix.

There are clearly two main parts to solve this problem. The first problem is to generate synthetic data from a model (the forward problem) and the second is to find an efficient method for solving the minimization of equation.

Forward Problem

The 2D elastic forward modeling was carried out using a fourth-order in space, second-order in time, finite difference method (Levander, 1988). This was chosen due to consideration of the computational expense of more realistic modeling and the fact that the salt is relatively isotropic and has much lower attenuation than most rock types. Optimally absorbing boundaries were used to damp energy reaching the sides of the grid (Peng and Toksöz, 1995). In time-domain modeling, using a point source, during early times the wavefield is confined to a small area in the proximity of the source, the speed at which this area grows depends on the velocities. As this area is much smaller than the total grid size, an expanding grid strategy was used to save computational time. For further details on the forward modeling and expanding grid strategy see Shipp and Singh (2002). This modeling approach can be considered as an operator (g) operating on the model (m) to produce the synthetic data: $d_{syn}(s, r, t) = g(m)$.

Inverse Problem

We perform the inversion by using the conjugate gradient method. The explicit calculation of the partial derivatives for the gradient calculation (known as Fréchet derivatives) is relatively expensive. Fortunately, the gradient can be solved using the adjoint state approach which results in an equation similar to the imaging condition in pre-stack depth migration and is a function of two separate wave-fields (Tarantola, 1986). The first being the modeled forward wave-field and the second represents a wave-field in which the receiver positions become source locations and the source-signature of these sources being the difference between the real and synthetic data at each point and in reverse time. This can be considered as representing the *residual* or missing wave-field, representing energy that was absent in the forward modeling step with the current model.

In waveform inversion there is a problem of coupling between parameters. It has been shown that for long offsets and transmitted data the velocities are the parameters that are least coupled in the inversion and so are suitable parameters to invert for, whereas for short offset and reflection data the P-wave and S-wave impedances are more suitable parameters (Tarantola, 1986). In this case, both the transmitted and reflected arrivals play an important role. As the transmitted arrivals are the dominant arrivals we have chosen to invert for the velocities. Ideally, we would invert for the velocities in the region of the model above the receiver array and for the impedances beneath the array. However, this would lead to complications in the transition zone. The conjugate gradient can then be found using a simple combination of the gradient directions at the current and previous iteration and the conjugate gradient at the previous iteration (Polak, 1971).

Having established a search direction it is now necessary to step-length (the magnitude of the update) this is done by performing a small perturbation to the current model in the direction of the update as described by Pica et al. (1990). This simple step-length calculation is used due the cost of the forward modeling operation and the resulting cost of performing a line search. This procedure is performed until some criteria is reached (here it is for a finite user specified number of iterations limited by computational time).

Multi-scale Approach

Due to the non-linearity of the forward problem and the size of the problem, waveform inversion may converge to a local minimum. One principle cause of this is the cycle skipping that occurs when an event in the data, generated from the starting model, is at a temporal distance greater than the period associated with the dominant frequency in the data. We take several steps to divide the problem at different scales.



For example, travel time tomography that is commonly used to get starting velocity models provides very long wavelength information. In order to get the medium wavelength information, we first invert long offset data, and then move towards near offset data. To further reduce the problem of cycle skipping a low pass filter is applied which makes each cycle longer in time and so decreases the accuracy to which the starting model must match arrivals for the inversion to converge to the global minimum. The inversion is then performed first for the lowest frequencies contained in the data and then performed for progressively higher frequencies as convergence to the global minimum approached. Since the near surface structures are independent on deep structures (reverse is not true), we first invert for near surface structure and then invert deeper structure. First we invert V_z field to determine P-wave velocity. Then we invert S-wave from V_z in order to get medium-scale S-wave velocity information and then we finally invert V_x data to get fine-scale S-wave velocity. This also reduces the computational burden as a larger grid size and time step can be used at different steps. Finally, all the data and all the frequencies are inverted simultaneously in order to get a globally consistent model.

We have extensively tested our algorithm to different synthetic data sets and have applied to several data with different acquisition geometry and complexity of the problems. Here we will present three examples that demonstrate the potential of our waveform inversion technique.

Inversion of OBC Data

We have applied the waveform inversion to a 2-D OBC line from the Alba Field, UK Central North Sea. The Alba Field is an Eocene turbidite sand reservoir, located at around 2 km depth (MacLeod et al., 1999). Figure 1 shows example of vertical (V_z) and horizontal (V_x) wavefield. Prior to drilling showed a bright spot, which was an outlier sands.

The starting P-wave velocity model was based on a depth converted time-RMS velocity field, provided by Chevron. A starting S-wave velocity model was generated using empirical relationships. A source wavelet was extracted from the dataset, for the finite-difference modelling. The OBC geometry allows stacking of true zero-offset direct arrivals, preferred for source estimation.

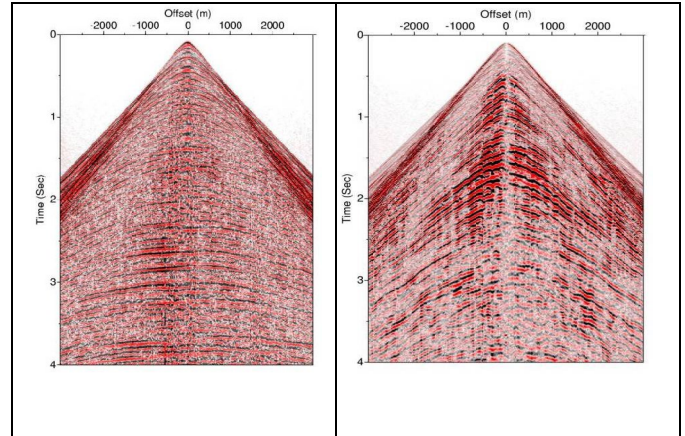


Figure 1: Example raw vertical and horizontal (inline) geophone gathers from Alba Field, with simple $t^{2.0}$ and $t^{1.8}$ gains applied respectively, for display purposes. PS events can suffer from shear wave static problems.

Using P-wave data on the V_z component, inversion for P- and S-wave velocity was undertaken in a two stage processes as mentioned before. Inversion for the more dominant P-wave velocity in the first stage was followed by inversion for S-wave velocity, exploiting the residual AVO response of P-wave events for S-wave velocity information. Further updates to P-wave velocity were also permitted, although small. P-wave velocity results in Figure 2 show encouraging results. Note the distinct field outlines visible around 2 km depth. However, a decrease in P-wave velocity is associated with the reservoir. From limited nearby well data, it was found that the hydrocarbon bearing Alba sands are marked by a decrease in density and increase in wave velocities, compared to adjacent layers.

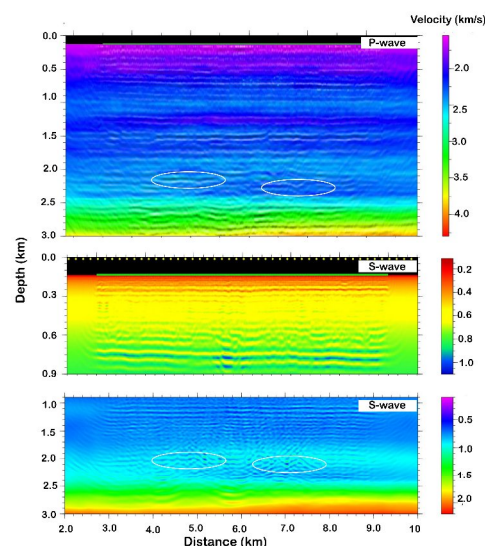


Figure 2: Inverted P-wave (top) and S-wave velocities (middle and bottom). Alba gas field is marked by white ellipses.



To overcome computational limitations, inversion of S-wave data was achieved in two steps: 1) a shallow model down to 1 km depth, using a fine grid ($dx=1.25m$) and low S-wave velocity at the seabed; 2) a deep model down to 3 km depth, using a more computationally feasible coarse grid ($dx=4.16m$) but fixing the shallow seabed Vs to an average value of $312ms^{-1}$. The shallow model inversion was of interest for resolving the seabed region, of interest for static problems in conventional processing or detection of drilling hazards (overpressure) (Figure 2 middle). Note the short scale features of S-wave velocity recovered when using low temporal frequency S-wave data.

Inversion for deeper targets showed similarly high spatial resolution from low frequency data. Features associated with the Alba reservoir, 4.4 – 5.4 km and 6.2 – 7.2 km, can be seen, including a distinct wing-like edge. Note again the high spatial resolution achieved despite low temporal frequencies used.

Inversion Of Walk-Away VSP Data

Drilling beneath salt in the deep-water Gulf of Mexico (GOM) is an expensive and potentially hazardous activity due to the presence of high-pressure fluid. Quantitative knowledge of the P-wave and S-wave velocities (or their ratio) can be useful in predicting the pore pressure in the sedimentary layer below the base of the salt, providing useful information for planning a salt exit drilling fluid strategy to reduce the risks involved in drilling. Reliable velocity prediction below salt is difficult due to the depths involved, the complex structure of salt domes and the high seismic velocity of the salt. To overcome some of these difficulties, the use of walk-away VSP data has been applied, whereby the drilling is stopped in the salt layer, normally to make a casing run, and a VSP survey is shot with receivers in the salt. This type of survey has the advantage of sampling the wave-field beneath the top salt and having the receiver much nearer the target thus containing much greater reflection energy from the sub-salt sediments.

We applied our 2D waveform inversion to recover the elastic parameters in the sedimentary layer beneath the salt from a walk-away VSP (vertical seismic profile) carried out with the receivers in the salt, with the objective of estimating pore pressure at the base of salt.

Ten three component receivers, spaced at 150 m were deployed between 4.5 and 5.85 km depth. The source was modeled at 12.5 m depth and repeated at 50 m intervals. 319 shots were used with offsets from 7.75 km before the receiver array to 8.15 km after the array. The reciprocity theory was used to minimize the computational requirements enabling us to perform a modeling operation for every receiver rather than for every shot.

The inversion was performed in a multi-scale scheme, whereby 15 iterations were performed with data low pass filtered at each of the following frequencies: 6, 9, 12 & 15 Hz. The output model from a given inversion was used as a starting model for the next frequency band. A cut-out mute was applied to the data to remove the first water bottom multiple and a lower mute was applied above the second multiple, as these were large amplitude events that had an adverse effect on the inversion. The source was estimated using the approach described above and was estimated on the filtered data at each frequency range. As density was not inverted for, the density was linked to the P-wave velocity model at the beginning of each inversion

Figure 3 shows the results of waveform inversion. At the base of the salt the P-wave velocity decreases from 4.8 km/s to 3.5 km/s, suggesting the presence of sediments, whereas S-wave decreases from 3 km/s to 1.0 km/s. The large decreases in S-wave velocity seems to be associated with high fluid pressure, which was confirmed by later drilling. The velocities obtained by our inversion were close to the drilling results. Our results also show sedimentary structures beneath the salt.

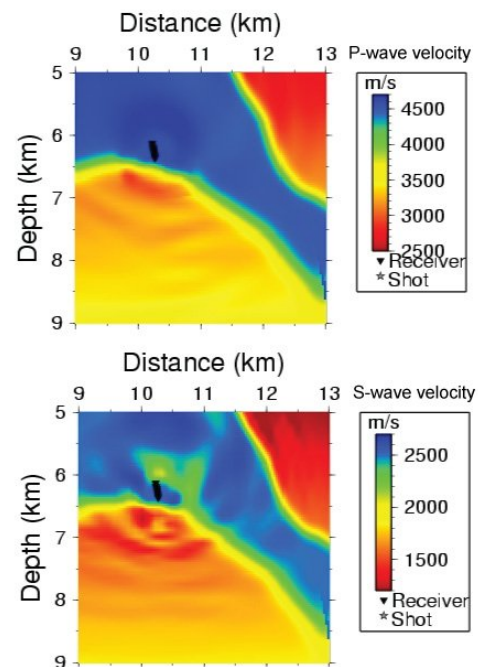


Figure 3: Results of waveform inversion of multi-component walk-away VSP data from the Gulf of Mexico. A decrease on both P-wave (top) and S-wave velocity is observed beneath the salt (high velocity, blue). Inversion also indicates sediment layering beneath the salt, which was not possible to image using surface seismic.



Inversion in Time-Lapse Mode

For time-lapse seismic, 3D seismic data are acquired at different times using acquisition parameters as close as possible, data are processed using similar processing sequences, final images are cross-equalized, and are subtracted from the base line image to obtain 4D image. The differences in acquisition, processing from one vintage to the other, and long wavelength variation due to change in velocity and cycle skipping would be mapped in to 4D image. Furthermore, the 4D image is qualitative. In order to remove these effects, we propose to apply full waveform inversion to different data vintages, and instead of comparing the data image, we compare inverted model, which provides the changes in velocities. We have applied this technique to monitor CO₂ sequestration in the North Sea.

Sleipner oil field is situated in the Norwegian sector of the North Sea. The deep oil (3 km) contains a significant amount of CO₂. Instead of ejecting CO₂ in the atmosphere, the CO₂ is separated and injected in a saline aquifer at 700-1000 m depth in Utsira sands. The aquifer consists of thin beds (10 m) of Utsira sands and shale (5 m), with a thick shale layer forming the cap rock.

The first 3D seismic reflection data was acquired in 1994. First CO₂ underground storage began on this North Sea site in 1996. Since then 3D seismic data were acquired in 1999, 2001, 2004, and 2006. We have access to 1994, 1999 and 2006 vintage.

Inversion of pre-injection data (1994) was carried out using a frequency cascading approach where result for a given frequency range is used as starting model for the next higher one. The very first initial model is a smoothed version of the background velocity model. Only P velocities were directly inverted, S velocity is linked to P-wave velocity. Dozens of iterations were performed for each run, to insure satisfying convergence. Frequency cascading allows stabilizing the inverse problem by inverting the more linear component (low frequencies) of the signal first.

The result of pre-injection data (1994) inversion was used as initial model for the post-injection data (1999, 2006) inversion. To insure stability of the overburden (supposed to be correctly estimated from pre-injection data), the part overlying the injected area is frozen. Furthermore, we consider that S wave velocities and density remain (almost) constant after gas injection. Consequently, S velocity and density model obtained by pre-injection data inversion were frozen during post-injection data inversion. Moreover, P wave velocities are supposed to decrease with gas injection.

The difference in P-wave velocity between pre-injection (1994) and post-injection (2006) are shown in Figure 4. The results clearly show that there is a significant decrease in P-wave velocity due to CO₂ injection, and layers of 10 m thick have been identified. The ringing, which was present in the 4D image, has been reduced as inter-bed multiples have been modelled correctly. The velocity differences between 1994 and 1999 and 1994 and 2006 inverted models could provide amount of in solution and in the form of free gas.

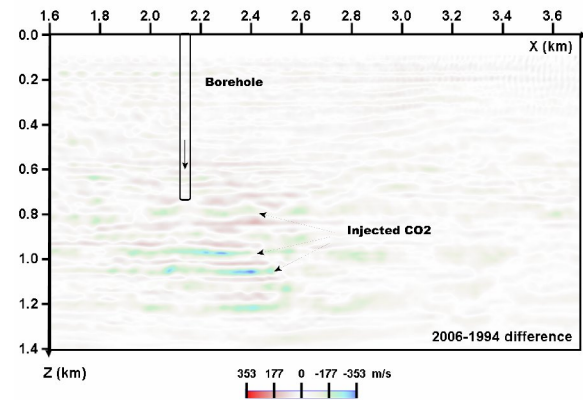


Figure 4: The difference in P-wave velocity between pre-injected (1994) and post-injected (2006). The maximum decrease in velocity is of the order of 400 m/s.

Conclusions

We have demonstrated that 2D elastic full waveform inversion is feasible and provide quantitative information on P and S-wave velocities. Our inversion method is robust and could be applied to complex problems where the velocity contrast is on the scale of >1 km/s. The inversion of V_z component data provides medium-scale information S-wave velocity whereas the inversion of V_x data provides very fine-scale information on S-wave velocity. The inversion could be used in time-lapse mode, providing quantitative 4D image. Our results show that the quantitative seismic imaging is feasible using elastic full waveform inversion. We plan to apply our method to Life Of the Field 4C (LoF) surveys so that the detailed fluid and pressure movement could be monitored.

Reference

Freudenreich, Y., Singh S. and Barton, P. 2001, Sub-basalt imaging using a full elastic wavefield inversion scheme, 63rd Mtg. Eur. Assn. of Expl. Geophys., Session O-19



Levander, A. 1988, Fourth-order finite-difference P-SV seismograms, *Geophysics*, 53, 1425-1436

Peng, C. and Toksöz, M. N., 1995, An optimal absorbing boundary condition for elastic wave modelling: *Geophysics*, **60**, 296–301.

Pica, A., Diet, J. P., and Tarantola, A., 1990, Nonlinear inversion of seismic reflection data in a laterally invariant medium: *Geophysics*, **55**, 284–292.

Polak, E., 1971, *Computational methods in optimization: A unified approach*: Academic Press.

Shipp, R.M. and Singh, S.C. 2002, Two-dimensional full wavefield inversion of wide-aperture seismic streamer data, *Geophys. J. Int.*, 151, 325-344

Singh, S.C., Kent, G., Collier, J., Harding A. and Orcutt J. 1998, Melt to Mush variations in the crustal magma properties beneath the Southern East Pacific Rise, *Nature*, 394, 874-878.

Singh, S.C., Minshull, T.A. and Spence, G.D. 1993, Velocity structure of a gas hydrate reflector, *Science*, 260, 204-206.

Tarantola, A. 1986, A strategy for non-linear elastic inversion of seismic reflection data: *Geophysics*, 1893–1903